Eur J Nucl Med Mol Imaging (2017) 44:392–397
DOI 10.1007/s00259-016-3585-0

SHORT COMMUNICATION

Intra-lesional spatial correlation of static and dynamic FET-PET parameters with MRI-based cerebral blood volume in patients with untreated glioma

Jens Göttler[1,2] · Mathias Lukas[3] · Anne Kluge[1] · Stephan Kaczmarz[1] · Jens Gempt[4] · Florian Ringel[4] · Mona Mustafa[3] · Bernhard Meyer[4] · Claus Zimmer[1] · Markus Schwaiger[3] · Stefan Förster[2,3,5] · Christine Preibisch[1,2] · Thomas Pyka[3]

Received: 13 September 2016 / Accepted: 22 November 2016 / Published online: 2 December 2016

Abstract
Purpose ^{18}F-fluorethyltyrosine-(FET)-PET and MRI-based relative cerebral blood volume (rCBV) have both been used to characterize gliomas. Recently, inter-individual correlations between peak static FET-uptake and rCBV have been reported. Herein, we assess the local intra-lesional relation between FET-PET parameters and rCBV.
Methods Thirty untreated glioma patients (27 high-grade) underwent simultaneous PET/MRI on a 3 T hybrid scanner obtaining structural and dynamic susceptibility contrast sequences. Static FET-uptake and dynamic FET-slope were correlated with rCBV within tumour hotspots across patients and intra-lesionally using a mixed-effects model to account for inter-individual variation. Furthermore, maximal congruency of tumour volumes defined by FET-uptake and rCBV was determined.
Results While the inter-individual relationship between peak static FET-uptake and rCBV could be confirmed, our intra-lesional, voxel-wise analysis revealed significant positive correlations (median $r = 0.374$, $p < 0.0001$). Similarly, significant inter- and intra-individual correlations were observed between FET-slope and rCBV. However, rCBV explained only 12% of the static and 5% of the dynamic FET-PET variance and maximal overlap of respective tumour volumes was 37% on average.
Conclusions Our results show that the relation between peak values of MR-based rCBV and static FET-uptake can also be observed intra-individually on a voxel basis and also applies to a dynamic FET parameter, possibly determining hotspots of higher biological malignancy. However, just a small part of the FET-PET signal variance is explained by rCBV and tumour volumes determined by the two modalities showed only moderate overlap. These findings indicate that FET-PET and MR-based rCBV provide both congruent and complimentary information on glioma biology.

Keywords ^{18}F-fluorethyltyrosine-PET · DSC MRI · CBV · Glioma

Electronic supplementary material The online version of this article (doi:10.1007/s00259-016-3585-0) contains supplementary material, which is available to authorized users.

✉ Jens Göttler
jens.goettler@tum.de

[1] Department of Neuroradiology, Klinikum rechts der Isar, TU München, Ismaninger Str. 22, 81675 Munich, Germany

[2] TUM Neuroimaging Center (TUM-NIC), Klinikum rechts der Isar, TU München, Ismaninger Str. 22, 81675 Munich, Germany

[3] Department of Nuclear Medicine, Klinikum rechts der Isar, TU München, Ismaninger Str. 22, 81675 Munich, Germany

[4] Department of Neurosurgery, Klinikum rechts der Isar, TU München, Ismaninger Str. 22, 81675 Munich, Germany

[5] Department of Nuclear Medicine, Klinikum Bayreuth, Preuschwitzer Str. 101, 95445 Bayreuth, Germany

Introduction

While conventional MRI is considered the gold standard for morphologic imaging of brain tumours, biological characterization of lesions, e.g. for pre-operative tumour grading or to differentiate recurrence from post-therapeutic changes is challenging. MRI-based relative cerebral blood volume (rCBV) obtained by dynamic susceptibility contrast (DSC) has been shown to improve the work-up of glioma with respect to these diagnostic difficulties as it is able to detect viable tumour tissue by its abnormal neovasculature [1]. Similar abilities

have been demonstrated for PET imaging with amino acid tracers, such as ^{18}F-fluoroethyltyrosine (FET), making use of the increased amino acid uptake in most gliomas relative to healthy brain tissue [2].

With the advent of integrated PET/MRI, both DSC and FET-PET can now be performed simultaneously in one single examination, which improves patients' convenience and might further increase the diagnostic accuracy due to the multiparametric analysis. However, data on the inter-dependency of the two modalities is inconsistent; few studies have shown significant correlations between maximum rCBV and static FET-PET uptake in different lesions but poor congruency of tumour volumes [3, 4], other studies with methionine PET demonstrated good correspondence of tumour hotspots defined by methionine uptake and rCBV [5–7]. It is still unclear, though, to which degree congruency exists on a regional or single voxel level, a matter of interest for the delineation of regions of higher malignancy or vital tumour tissue after treatment. Furthermore, the up-to-now available data did not fully include dynamic FET parameters, which are supposed to increase the diagnostic accuracy of FET-PET imaging further [8]. In this study, we take advantage of the favourable temporal and spatial co-registration of simultaneously acquired FET-PET/MRI, analysing the inter- and intra-individual correlation of rCBV and static and dynamic FET-PET parameters, in order to provide a framework for multi-modal, multi-parametric imaging of gliomas in the future.

Material and methods

Participants

We retrospectively analysed 30 patients (age 57.8 ± 16.8 years, 26 men) with suspected glioma who were enrolled in a study on pre-therapeutic characterization of gliomas from Feb. 2013 until Jul. 2015. The study was approved by the local ethics committee (vote 5547/12). Informed consent was obtained from all individual participants. Histological analysis after biopsy or resection revealed 23 patients with WHO °IV (all glioblastoma multiforme), four patients with WHO °III (anaplastic astrocytoma in two cases and anaplastic oligodendroglioma in one case, not specifiable in one case), and three patients with WHO °II (astrocytoma in one case and oligoastrocytoma in two cases) glioma.

For detailed description of the acquisition protocol, see supplementary material.

PET/MR image analysis

All image processing was done using MATLAB (MathWorks, Natick, MA, USA) and SPM (Wellcome Department of Cognitive Neurology, London, UK).

FET-PET

Static FET images 10–20 and 30–40 min post-injection (p.i.) were resampled and co-registered onto each subject's contrast-enhanced MPRAGE sequence using SPM8; subsequently, they were normalized to the mean tracer uptake in a 1.5 cm circular region in grey matter of the non-tumour-bearing hemisphere (VOL_{Ref}), resulting in tumour-to-background ratios (TBRs). FET tumour volume was defined on a TBR isocontour of 1.6 ($VOL_{Tumour,FET}$) according to [9]. Hotspots of FET-uptake were defined using a 90% isocontour around the voxel with maximum FET-uptake in the tumour ($VOL_{Peak,FET}$). Time-activity-curves were determined on the dynamic SUV images in single voxels. On the time-activity curve data, we calculated the curve slope (SUV/h) from 10 to 30 min p.i. resulting in a FET activity slope map for each lesion.

DSC

CBV maps were calculated using an established protocol [10] and normalized to normal-appearing white matter of the contralesional hemisphere. Resulting rCBV maps were resampled and co-registered in the same way as PET images (Fig. 1). Peak values where determined by a 5 mm circular VOI around the voxel with the maximum rCBV value within the tumour ($VOL_{Peak,rCBV}$).

Multimodal analysis

Tumour hotspots of FET-uptake and rCBV were localized for all gliomas and their distance was calculated. To compare the TBR of CBV and FET-uptake, we divided the mean value within $VOL_{Tumour,FET}$ by the mean value within VOL_{Ref} in each patient. Furthermore, peak values of FET-PET (static uptake and slope) and rCBV in the tumour as well as averaged values for $VOL_{Tumour,FET}$ and $VOL_{Peak,FET}$ were correlated across all patients using SPSS 23 (IBM Corp., Armonk, NY, USA), obtaining Pearson correlation coefficients. Within $VOL_{Tumour,FET}$, the respective parameters were compared voxel-wise using Pearson correlation and linear regression. In order to account for inter-individual variation, a linear mixed-effects model was employed as follows:

$$PET_{im} = \beta_0 + \beta_1 rCBV_{im} + b_{0m} + b_{1m} rCBV_{im} + \varepsilon_{im} \quad (1)$$

where $rCBV_{im}$, PET_{im} represent rCBV and PET (normalized early uptake, late uptake, or slope) measurements of voxel i in patient m, β denoting fixed effects, and b and ε representing normally distributed random (i.e. patient-specific) effects and observation errors. A two-tailed significance level of 0.05 was applied for all tests.

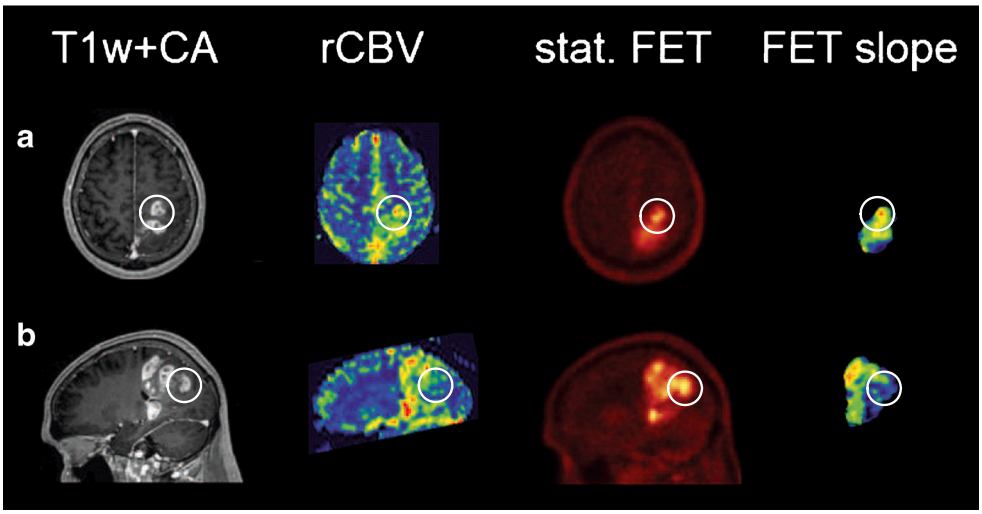

Fig. 1 Coregistered maps of rCBV, static FET-uptake and FET-slope maps. Image example of two patients with glioblastoma: coregistered maps of relative cerebral blood volume (rCBV), early static normalized FET-uptake (10-20 min p.i.), and FET-slope together with a contrast enhanced MPRAGE sequence (T1w + CA). **a** Good correspondence of all modalities. **b** Tumour region with obvious FET-uptake but lacking rCBV increases and slope reductions

In order to determine cut-off values for rCBV for which the resulting tumour volume ($VOL_{Tumour,rCBV}$) corresponded best with the one defined by FET-uptake with a tumour-to-brain ratio of 1.6 ($VOL_{Tumour,FET}$), we calculated the Dice coefficient (DC) [4] for variable thresholds of rCBV within a spherical volume comprising all FLAIR-hyperintensities surrounding the tumour using a MATLAB-based script.

Results

The mean distance between the tumour hotspots of FET-uptake and rCBV was 20.0 +/− 14.1 mm. Mean TBR of early and late FET-uptake was significantly higher than TBR of CBV (2.5 +/− 0.6 and 2.2 +/− 0.5 vs. 1.4 +/− 0.5, $p < 0.0001$). Peak values of early FET-uptake from 10 to 20 min p.i. showed higher correlations to rCBV than late FET-uptake measured from 30 to 40 min, while both correlations were significant (r = 0.529, $p = 0.003$ and r = 0.430, $p = 0.018$, Table 1), respectively. Furthermore, peak rCBV was also correlated significantly with dynamic FET-slope (r = −0.592, $p < 0.001$, Table 1), with negative correlation coefficients as expected. Similar results could be demonstrated when only the region of peak PET signal ($VOL_{Peak,FET}$) was evaluated (Table 1, Fig. 2a). When calculating and comparing average values over $VOL_{Tumour,FET}$, correlations between rCBV and static FET signal were considerably weaker, while averaged dynamic FET-slope was still highly significantly correlated to the average rCBV (r = 0.702, $p < 0.001$, Table 1, Fig. 2c).

Table 1 Inter-individual correlation between rCBV and FET-PET parameters

Volume		FET10-20	FET30-40	FET-slope
$VOL_{Peak,FET\&rCBV}$	r	0.529	0.430	−0.592
	p	0.003	0.018	<0.001
$VOL_{Peak,FET}$	r	0.576	0.447	−0.603
	p	0.001	0.013	<0.001
$VOL_{Tumour,FET}$	r	0.470	0.215	−0.702
	p	0.009	0.254	<0.001

Voxel-wise comparison of FET-PET to rCBV within $VOL_{Tumour,FET}$ confirmed a positive correlation between rCBV and static FET-uptake (Fig. 2b). For early PET measurements median Pearson's r was 0.355 (Fig. 3), mean gradient (β_1) and intercept (β_0) for the prediction of early PET uptake by rCBV (fixed effects) were 0.113 ($p < 0.0001$) and 1.871 (Table S1, supplementary material). For late PET measurements, the association was slightly weaker (r = 0.328; β_1 = 0.084, $p < 0.0001$; $\beta_0 = 1.951$). Similar to inter-individual analysis, a negative correlation between FET-slope and rCBV could be shown intra-lesionally (r = −0.225; β_1 = −0.108, $p < 0.0001$; $\beta_0 = 0.371$; Fig. 2d). The proportion of the FET-PET signal variance explained by rCBV (median R^2, 25 and 75 percentile in parentheses) was 0.129 (0.071–0.220) for early FET-uptake, 0.107 (0.045–0.211) for late FET-uptake and 0.056 (0.020–0.124) for FET-slope.

The maximal overlap of tumour volumes as defined by FET-uptake (TBR > 1.6) and rCBV was approx. 37% (median DC) at a cut-off value of rCBV = 2.84 (Fig. 4).

Discussion

The aim of this study was to investigate the relation between rCBV, as assessed by DSC, and static and dynamic FET-PET at a hybrid PET/MRI scanner in order to investigate a promising diagnostic framework for multi-modal, multi-parametric imaging in the clinical work-up and characterization of untreated glioma patients.

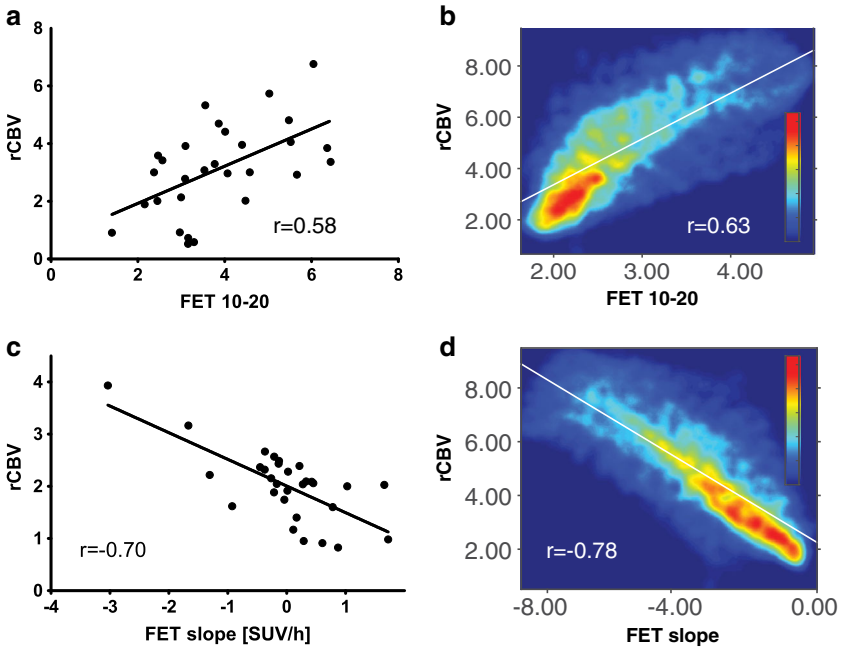

Fig. 2 Inter-individual (**a**, **c**) and voxel-wise, intra-lesional (**b**, **d**) correlation between FET-uptake and DSC-based rCBV. **a** Correlation of maximum early static FET-uptake with maximum rCBV in the tumour hotspots ($VOL_{Peak,FET}$) across all patients ($r = 0.576$, $p < 0.001$) **c** Correlation of averaged dynamic FET-slope and rCBV within a tumour volume defined on PET ($VOL_{Tumour,FET}$) across all patients ($r = -0.702$, $p < 0.001$). **b** and **d** Example scatter plot voxel-wise correlating early static FET-uptake and FET-slope, respectively, with rCBV values within $VOL_{Tumour,FET}$. High voxel densities are depicted in *red*, low densities in *blue* (colorbar)

First, we found that the TBR of FET-uptake was significantly higher than the TBR of CBV and the location of hotspots differed considerably, being in line with the literature [3]. Additionally, we confirmed results from previous studies, which had found significant associations between peak values of rCBV and static FET-PET uptake across all patients [3, 4]. We further revealed that rCBV is also correlated with a common dynamic PET parameter (slope of the time-activity-curve), which has been suggested to provide additional information on glioma biology. Most interestingly, we also found a clear intra-lesional spatial correlation of rCBV with static and dynamic FET parameters. These results provide first evidence that the spatial pattern of rCBV and FET-PET measures correspond within gliomas although they target different aspects of tumour biology: On the one hand, increases of rCBV within gliomas are thought to primarily reflect tumour-induced microvascular hyperplasia [1]. FET tracer uptake, on the other hand, visualizes the gliomas' trait to absorb higher amounts of amino acids than normal brain tissue within the same time, possibly due to an upregulation of amino acid transporters [11]. Some authors argue that highly malignant glioma tissue is supposed to exhibit both higher perfusion due to tumour neovascularisation and also increased amino acid uptake, which would explain at least a part of the observed correlation between the imaging modalities [3, 4]. However, FET-uptake, as far as it is described by common kinetic models [12], might be enhanced by perfusion effects itself since increased blood flow leads to elevated tracer "wash-in". This effect should be more pronounced in the early phase of the time-activity-curve as plasma levels of FET in the first 10 min p.i. are higher, also because urinary excretion of FET is rather slow [13]. Indeed, we found that early FET-PET summation images exhibited higher correlation coefficients with rCBV than late FET-PET images indicating that blood volume (i.e. tracer still located in the blood vessels) contributes to local early FET-PET activity. A negative slope, however, indicates that tracer "wash-out" from the tissue after having reached an activity peak is more pronounced in high-grade gliomas [14]. The correlation between FET wash-out and perfusion cannot easily be explained by a direct perfusion effect, as amino acid transporters involved in FET-uptake are supposed to allow only small amounts of tracer efflux [11].

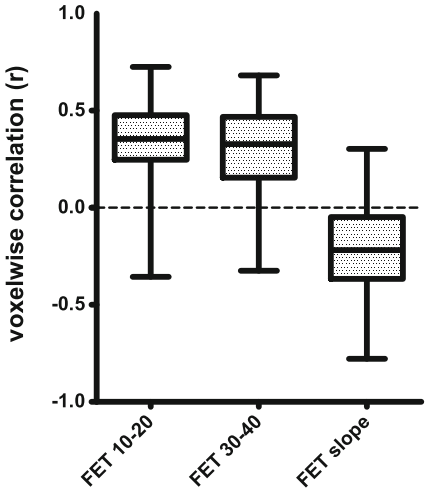

Fig. 3 Intra-individual correlation of FET-uptake and rCBV. Box plots depicting the range of intra-individual correlation coefficients between rCBV and early, late, and dynamic FET-PET parameters. The boxes contain all values between the first and third quartile, the *black line* inside marks the mean and the whiskers reach from minimum to maximum

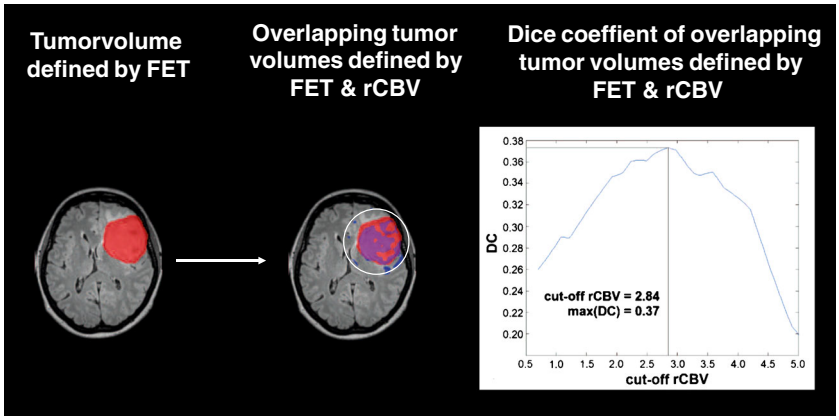

Fig. 4 Calculation of the Dice coefficient (DC) between tumour volumes defined by early FET-uptake and rCBV at variable cut-offs. Column 1: Tumour volume as defined by a tumour-to-brain ratio of 1.6 and above of static FET-uptake during 10–20 min p.i. (*red*) in a patient with left frontal glioblastoma. Column 2: Overlap of the tumour volume as defined by a FET (*red*) and by rCBV (*blue*) at the optimal threshold within a spherical VOI comprising all FLAIR-hyperintensities. Column 3: Relationship of the DC between the tumour volumes as defined by FET-uptake (tumour-to-brain ratio of 1.6 and above) and rCBV at variable thresholds across all patients. Maximum overlap was achieved at an optimal rCBV cut-off of 2.84 yielding a DC of 0.37

That said, we found that only 13% of the variance of early and 11% of late uptake was explained by perfusion effects, i.e. rCBV. Even less variance of the time-activity-slope was accounted for by rCBV. Furthermore, we only found a moderate spatial overlap of tumour volumes as defined by static FET-uptake and rCBV even at an optimal cut-off for rCBV as determined by iterative DC analysis. This poor correspondence might in part be due to the relatively low tumour-to-brain contrast of CBV maps exhibiting equally increased values outside the tumour, e.g. in blood vessels or in the choroid plexus and their very noisy appearance also showing high variability between scanners and the used sequences. Additionally, the tumour volume of FET-uptake can also extend in some-rare-cases beyond FLAIR hyperintensities; however, this was not observed in our cohort. We decided not to define tumour volumes and a tumour-to-brain contrast for FET slope, as such a measure does not seem to be meaningful, i.e. zero slope can be found in tumour as well as healthy brain regions, and dynamic FET analysis in the literature focussed on the kinetics within hotspots.

In summary, our findings indicate that static and dynamic FET-uptake measures and rCBV as determined by DSC-MRI are interdependent and exhibit only a poor spatial overlap; therefore, the two modalities can certainly be assumed to depict different aspects of tumour biology. With simultaneous PET/MRI, it is possible to generate a more integrated picture of the tumour biology, which might provide a powerful diagnostic tool for localizing regions of higher malignancy, assessing response to radiochemotherapy, or detecting spots of recurrence. However, further studies are needed to determine the relative contributions of DSC-MRI and FET-PET with regard to these questions and to evaluate the clinical benefit from multi-modal, multi-parametric imaging of brain tumours.

Acknowledgements We thank Daniela Hiob (Technical University of Munich) for the careful revision of the manuscript.

Compliance with ethical standards All procedures performed in studies involving human participants were in accordance with the ethical standards of the institutional and national research committee and with the 1964 Helsinki declaration and its later amendments or comparable ethical standards.

Funding This study was supported by funding from the German Research Foundation DFG (grant to CP, SF and TP: FO 886/1-1; PR 1039/4-1) and from the Faculty of Medicine of the Technical University of Munich (grant to TP: KKF B11-14; and to JGö: KKF E12).

Conflict of interest The authors declare that they have no conflict of interest. BM and JGe report personal fees from Brain Lab AG, outside the submitted work.

References

1. Barajas Jr RF, Phillips JJ, Parvataneni R, Molinaro A, Essock-Burns E, Bourne G, et al. Regional variation in histopathologic features of tumor specimens from treatment-naive glioblastoma correlates with anatomic and physiologic MR Imaging. Neuro-Oncology. 2012;14:942–54. doi:10.1093/neuonc/nos128.
2. Dunet V, Rossier C, Buck A, Stupp R, Prior JO. Performance of 18F-fluoro-ethyl-tyrosine (18F-FET) PET for the differential diagnosis of primary brain tumor: a systematic review and Metaanalysis. J Nucl Med. 2012;53:207–14. doi:10.2967/jnumed.111.096859.

3. Filss CP, Galldiks N, Stoffels G, Sabel M, Wittsack HJ, Turowski B, et al. Comparison of 18F-FET PET and perfusion-weighted MR imaging: a PET/MR imaging hybrid study in patients with brain tumors. J Nucl Med: Off Publ Soc Nucl Med. 2014;55:540–5. doi:10.2967/jnumed.113.129007.
4. Henriksen OM, Larsen VA, Muhic A, Hansen AE, Larsson HB, Poulsen HS, et al. Simultaneous evaluation of brain tumour metabolism, structure and blood volume using [F]-fluoroethyltyrosine (FET) PET/MRI: feasibility, agreement and initial experience. Eur J Nucl Med Mol Imaging. 2015. doi:10.1007/s00259-015-3183-6.
5. Sadeghi N, Salmon I, Tang BN, Denolin V, Levivier M, Wikler D, et al. Correlation between dynamic susceptibility contrast perfusion MRI and methionine metabolism in brain gliomas: preliminary results. J Magn Reson Imaging: JMRI. 2006;24:989–94. doi:10.1002/jmri.20757.
6. Sadeghi N, Salmon I, Decaestecker C, Levivier M, Metens T, Wikler D, et al. Stereotactic comparison among cerebral blood volume, methionine uptake, and histopathology in brain glioma. AJNR Am J Neuroradiol. 2007;28:455–61.
7. Dandois V, Rommel D, Renard L, Jamart J, Cosnard G. Substitution of 11C-methionine PET by perfusion MRI during the follow-up of treated high-grade gliomas: preliminary results in clinical practice. J Neuroradiol. 2010;37:89–97. doi:10.1016/j.neurad.2009.04.005.
8. Albert NL, Winkelmann I, Suchorska B, Wenter V, Schmid-Tannwald C, Mille E, et al. Early static (18)F-FET-PET scans have a higher accuracy for glioma grading than the standard 20–40 min scans. Eur J Nucl Med Mol Imaging. 2016;43:1105–14. doi:10.1007/s00259-015-3276-2.
9. Pauleit D, Floeth F, Hamacher K, Riemenschneider MJ, Reifenberger G, Muller HW, et al. O-(2-[18F]fluoroethyl)-L-tyrosine PET combined with MRI improves the diagnostic assessment of cerebral gliomas. Brain J Neurol. 2005;128:678–87. doi:10.1093/brain/awh399.
10. Kluge A, Lukas M, Toth V, Pyka T, Zimmer C, Preibisch C. Analysis of three leakage-correction methods for DSC-based measurement of relative cerebral blood volume with respect to heterogeneity in human gliomas. Magn Reson Imaging. 2015. doi:10.1016/j.mri.2015.12.015.
11. Habermeier A, Graf J, Sandhofer BF, Boissel JP, Roesch F, Closs EI. System L amino acid transporter LAT1 accumulates O-(2-fluoroethyl)-L-tyrosine (FET). Amino Acids. 2015;47:335–44. doi:10.1007/s00726-014-1863-3.
12. Thiele F, Ehmer J, Piroth MD, Eble MJ, Coenen HH, Kaiser HJ, et al. The quantification of dynamic FET PET imaging and correlation with the clinical outcome in patients with glioblastoma. Phys Med Biol. 2009;54:5525–39. doi:10.1088/0031-9155/54/18/012.
13. Langen KJ, Hamacher K, Weckesser M, Floeth F, Stoffels G, Bauer D, et al. O-(2-[18F]fluoroethyl)-L-tyrosine: uptake mechanisms and clinical applications. Nucl Med Biol. 2006;33:287–94. doi:10.1016/j.nucmedbio.2006.01.002.
14. Popperl G, Kreth FW, Mehrkens JH, Herms J, Seelos K, Koch W, et al. FET PET for the evaluation of untreated gliomas: correlation of FET uptake and uptake kinetics with tumour grading. Eur J Nucl Med Mol Imaging. 2007;34:1933–42. doi:10.1007/s00259-007-0534-y.